

Mirror symmetry breaking and restoration: the role of noise and chiral bias

David Hochberg^{1,*}

¹*Centro de Astrobiología (CSIC-INTA), Carretera Ajalvir Kilómetro 4, 28850 Torrejón de Ardoz, Madrid, Spain*

(Dated: October 31, 2018)

The nonequilibrium effective potential is computed for the Frank model of spontaneous mirror symmetry breaking (SMSB) in chemistry in which external noise is introduced to account for random environmental effects. When these fluctuations exceed a critical magnitude, mirror symmetry is restored. The competition between ambient noise and the chiral bias due to physical fields and polarized radiation can be explored with this potential.

PACS numbers: 05.40.Ca, 11.30.Qc, 87.15.B-

Enantiomers are molecules that are nonsuperimposable complete mirror images of each other. A remarkable feature of Nature is that this mirror or chiral symmetry is broken in all biological systems, where processes crucial for life such as replication, imply chiral supramolecular structures, sharing the same chiral sign (homochirality) for all present living systems. These chiral structures are proteins, composed by aminoacids almost exclusively found as the left-handed enantiomers (L), and DNA, RNA polymers and sugars with chiral building blocks composed by right-handed (D) monosaccharides, and chiral amphiphiles forming membranes. This fact has led to the widespread perception that the presence of handed or chiral molecules is a unique signature of living systems. The emergence of this biological homochirality in the chemical evolution from prebiotic to living systems is a tantalizing enigma in the origin of life, as is the robustness of homochirality in actual living systems, and is a fascinating subject that has intrigued scientists from diverse backgrounds. Current reviews of the origin of homochirality can be found in [1, 2, 3, 4, 5, 6]. Previous hypotheses suggesting that homochirality emerged after the development of the primeval biological system [7], are being replaced by the widespread conviction that enantiomerically pure compounds are a prerequisite for the evolution of living species and that mirror symmetry breaking must have taken place before the emergence of life [8, 9, 10]. We adopt the latter viewpoint here.

Frank introduced a paradigmatic model for spontaneous mirror symmetry breaking (SMSB) and autocatalytic amplification in 1953 [11]. A variant [12] of this open-flow reaction scheme involves the two enantiomers L and D and an achiral reactant A (kept at constant concentration) and the following reaction steps, where the $k_{\pm i}$ denote the forward/reverse (\pm) rate constants: *Production of chiral compound* (k_1, k_{-1}): $A \leftrightarrow L, A \leftrightarrow D$, *autocatalytic amplification* (k_2, k_{-2}): $L + A \leftrightarrow L + L, D + A \leftrightarrow D + D$, and *mutual inhibition* (k_3): $L + D \rightarrow LD$. The heterodimer LD is removed from the system. Frank's model contains the fundamental

ingredients believed to be essential for mirror symmetry breaking and subsequent chiral amplification [13]. It can be elaborated by adding in polymerization side reactions [14, 15, 16, 17, 18] that can yield homochirality in populations of oligomers. The corresponding rate equations expressed in terms of the enantiomeric excess (ee) $\eta = ([L] - [D])/([L] + [D])$, the order parameter for mirror symmetry breaking, and the net chiral matter $\chi = [L] + [D]$ are:

$$\begin{aligned} d\eta/dt &= -2k_1 A\eta/\chi + (k_3 - k_{-2})\chi\eta(1 - \eta^2)/2 \quad (1) \\ d\chi/dt &= 2k_1 A - \chi^2[k_{-2} + (k_3 - k_{-2})(1 - \eta^2)/2] \quad (2) \\ &\quad + (k_2 A - k_{-1})\chi. \end{aligned}$$

These rate equations are deterministic, but more realistic treatments should take noise phenomena into account. The nature of such fluctuations can be internal as well as external to the chemical system. Intrinsic statistical fluctuations in η about the ideal racemic composition $[L] = [D]$ [19], as well as diffusion-limited noise present in spatially extended systems [20], are sufficient to tip the system over into one of its equally likely stable chiral states when $k_3 > k_{-2}$. For prebiotic scenarios, the coupling of reaction schemes such as this one to environmental effects (e.g., meteor impacts) is crucial for determining the role of early planetary environments and external disruptions on the emergence, if any, of homochirality [18].

This Letter has a two-fold purpose. On the one hand, we aim to establish analytically the impact of both environmental disturbances and chiral bias on chemical systems that lead to SMSB. These external effects can be modeled stochastically and lead one to consider stochastic differential equations [18]. Recently, we developed an analytic perturbation method for calculating potentials associated with a wide class of stochastic partial differential equations [21]. The potential is ideally suited for treating symmetry breaking phenomena in nonequilibrium systems. Hence, the second goal of this Letter is to demonstrate the computational utility of that method for a fundamental model of mirror symmetry breaking. The basic result is that ambient noise tends to restore mirror symmetry and homochirality is diminished, confirming independent numerical results [18].

Tree potential. For constant A , introduce dimension-

*Electronic address: hochbergd@inta.es

less time $\tau = (k_2A - k_{-1})t$, and we verify that when the rate of autocatalytic amplification exceeds the rate of monomer decay, χ changes more rapidly than the enantiomeric excess η . The system rapidly reaches a quasisteady state for χ ($d\chi/dt \approx 0$) and then the slow variable η evolves and the full system reaches its true steady state [22]. For this adiabatic regime, we then put $\chi \rightarrow \chi^*$ in Eq. (1), where χ^* denotes the quasisteady value for χ . We define the potential $V(\eta)$ [15] via $\frac{d\eta}{dt} = F(\eta) = -V'(\eta)$, and so obtain

$$\frac{V(\eta)}{b} = \frac{\eta^4}{4} + (r - \frac{1}{2})\eta^2 + v_0, \quad (3)$$

where v_0 is an integration constant, and where $b = \frac{1}{2}(k_3 - k_{-2})\chi^* > 0$, $r = a/b$ and $a = k_1A/\chi^* \geq 0$. For the scaled potential, r is the only free variable. This is plotted in Fig. 1 as a function of $-1 \leq \eta \leq 1$ and for $0 \leq r \leq \frac{1}{2}$. The absolute minima correspond to the asymptotic stable states of the chemical system and are located at $\eta = \pm\sqrt{1-2r}$. By varying r , we see how direct monomer production ($k_1 > 0$) tends to racemize the system, as the two chiral minima move continuously towards zero and coalesce at the origin when k_1A increases. Strict homochirality $|\eta| = 1$ holds only for $k_1A = 0$, otherwise, $k_1A > 0$ implies $|\eta| < 1$. For $r \geq \frac{1}{2}$, the chiral symmetric state $\eta = 0$ is the only stable solution. Gleiser

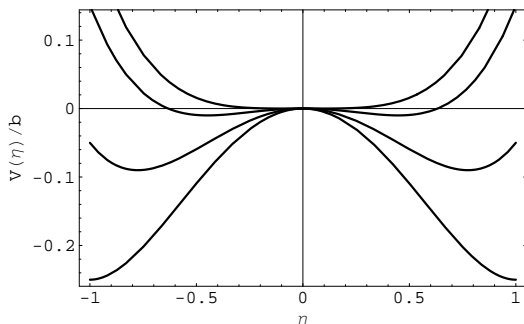


FIG. 1: The Frank model potential $V(\eta)/b$, Eq.(3), displaying the racemizing tendency of the direct chiral monomer production $A \rightarrow L$, $A \rightarrow D$. Sequence of curves from bottom to top: $r = 0, 0.2, 0.4$ and $r = 0.5$.

and Walker [18] obtained a potential qualitatively similar to Fig. 1, for a reduced polymerization model with direct production of monomers, which also clearly exhibits the racemizing tendency of such autogenic terms (see their Fig. 1a).

The effective potential. Following Gleiser and coworkers [18], we couple the system to an external noise source ξ to model random environmental effects. Applying the methods developed in [21], the corresponding stochastic differential equation for η

$$\frac{d\eta}{dt} = F(\eta) + \xi(t), \quad \langle \xi(t)\xi(t') \rangle = \mathcal{A} \delta(t - t'), \quad (4)$$

can be written as an ordinary differential equation with

an *effective*, noise-corrected force $F_{\mathcal{A}}$, as follows :

$$\frac{d\eta}{dt} = F_{\mathcal{A}}(\eta), \quad (5)$$

where to one-loop order in the noise amplitude \mathcal{A} , $F_{\mathcal{A}}$ is given by [21]

$$F_{\mathcal{A}}(\eta) = F(\eta) + \frac{1}{2} \frac{\mathcal{A}}{F(\eta)} \left(\Re \sqrt{[F'(\eta)]^2 + F(\eta)F''(\eta)} - \sqrt{[F'(\eta)]^2} \right) + O(\mathcal{A}^2), \quad (6)$$

and \Re is the real part. Thus for example, if a large meteor impacts near a well-mixed prebiotic puddle or small pond, the bulk pond is "shaken" as a whole and a time dependent noise $\xi(t)$ could provide a satisfactory description of the disturbance.

Eq.(3) for $r = 0$ implies $F(\eta) = b\eta(1 - \eta^2)$. The expression under the first square root in Eq.(6) is $[F'(\eta)]^2 + F(\eta)F''(\eta) = b^2(1 - 12\eta^2 + 15\eta^4)$. This is *negative* on the open intervals $(-0.84, -0.31)$ and $(0.31, 0.84)$, zero on their endpoints, and is strictly positive elsewhere [23].

The one-loop effective potential is therefore given by

$$V_{\mathcal{A}}(\eta) = - \int F_{\mathcal{A}}(\eta) d\eta + v_1, \quad (7)$$

where v_1 is an integration constant. We define

$$\mathcal{I}_1 = \int \frac{d\eta}{F(\eta)} \sqrt{[F'(\eta)]^2 + F(\eta)F''(\eta)}. \quad (8)$$

This integral can be worked out in closed form and yields

$$2\mathcal{I}_1 = -\ln \left| \frac{2\sqrt{R} - 12\eta^2 + 2}{\eta^2} \right| + 2 \ln \left| \frac{4\sqrt{R} + 18(\eta^2 - 1) + 8}{\eta^2 - 1} \right| - \sqrt{15} \ln |2\sqrt{15R} + 30\eta^2 - 12|, \quad (9)$$

valid whenever $R = 1 - 12\eta^2 + 15\eta^4 \geq 0$. Otherwise, from \Re in Eq.(6) we have $\mathcal{I}_1 = 0$. Next, define \mathcal{I}_2 as follows:

$$\mathcal{I}_2 = \int \frac{d\eta}{F(\eta)} \sqrt{[F'(\eta)]^2}. \quad (10)$$

Since the function $\sqrt{[F'(\eta)]^2} = b|(1 - 3\eta^2)|$ then \mathcal{I}_2

$$= \begin{cases} \frac{1}{2} \ln |\eta^2| + \ln |1 - \eta^2| + c_1, & (-\frac{1}{\sqrt{3}} < \eta < \frac{1}{\sqrt{3}}) \\ -\frac{1}{2} \ln |\eta^2| - \ln |1 - \eta^2| + c_2, & (\eta \leq -\frac{1}{\sqrt{3}} \ \& \ \frac{1}{\sqrt{3}} \leq \eta). \end{cases} \quad (11)$$

Matching up at $\eta^2 = \frac{1}{3}$ ensures continuity in \mathcal{I}_2 . Without loss of generality, we take $c_2 = 0$. Then $c_1 = -\ln \frac{1}{3} - 2 \ln \frac{2}{3} \simeq 1.91$.

The effective potential Eq.(7) can be written in terms of these two integrals as follows:

$$V_{\mathcal{A}}(\eta) = V(\eta) - \frac{\mathcal{A}}{2} \{ \mathcal{I}_1 - \mathcal{I}_2 \} + O(\mathcal{A}^2), \quad (12)$$

up to constants of integration used to match up the one-loop corrections to insure continuity. For domains over which $R \geq 0$, namely $\eta < -0.84$, and $-0.31 < \eta < 0.31$ and $\eta > 0.84$, then \mathcal{I}_1 is given by Eq.(9), otherwise when $R < 0$, then $\mathcal{I}_1 = 0$. Thus, for those regions over which $R < 0$, the one-loop correction in Eq.(12) is equal to $+\frac{A}{2}\mathcal{I}_2$. On the two outer intervals $(-1, -0.84)$ and $(0.84, 1)$, the one-loop correction is given by $-\frac{A}{2}\{\mathcal{I}_1 - \mathcal{I}_2\}$. From Eqs.(9,11) we can calculate this quantity valid on these intervals, and find that

$$\begin{aligned} \{\mathcal{I}_1 - \mathcal{I}_2\} &= -\frac{1}{2} \ln \left| \frac{2\sqrt{R} - 12\eta^2 + 2}{\eta^2} \right| + \frac{1}{2} \ln |\eta^2| \\ &+ \ln |4\sqrt{R} + 18(\eta^2 - 1) + 8| \\ &- \frac{\sqrt{15}}{2} \ln |2\sqrt{15R} + 30\eta^2 - 12|. \end{aligned} \quad (13)$$

Whereas for the central interval $(-0.31, 0.31)$, we calculate

$$\begin{aligned} \{\mathcal{I}_1 - \mathcal{I}_2\} &= -\frac{1}{2} \ln |2\sqrt{R} - 12\eta^2 + 2| - \ln |1 - \eta^2| - c_1 \\ &+ \ln \left| \frac{4\sqrt{R} + 18(\eta^2 - 1) + 8}{\eta^2 - 1} \right| \\ &- \frac{\sqrt{15}}{2} \ln |2\sqrt{15R} + 30\eta^2 - 12|. \end{aligned} \quad (14)$$

Next write $V_{\mathcal{A}} = V + (\mathcal{A}/2)\Delta V$, then the form of the pure one-loop correction $\Delta V(\eta)$ is completely specified as follows:

$$\Delta V(\eta) = \begin{cases} \delta V_{out}(\eta) + v_1 : & (-1, -0.84) \\ \mathcal{I}_2(\eta) + v_2 : & (-0.84, -0.31) \\ \delta V_{in}(\eta) + v_3 : & (-0.31, 0.31) \\ \mathcal{I}_2(\eta) + v_2 : & (0.31, 0.84) \\ \delta V_{out}(\eta) + v_1 : & (0.84, 1). \end{cases}$$

Here, $-\delta V_{out}$ is given by Eq.(13), $-\delta V_{in}$ by Eq.(14) and \mathcal{I}_2 by Eq.(11). Matching up at the endpoints of the above intervals fixes the constants $v_2 = v_1 + 3.182$, $v_3 = v_1 - 0.001$, where v_1 is an overall integration constant we are free to choose; see Eq.(7). We take $v_1 = \delta V_{in}(0)$.

Racemization. We investigate the role that weak external noise has on mirror symmetry breaking using the effective potential. We first scale out by the factor b , and evaluate $V_{\mathcal{A}}/b$ while varying the dimensionless noise amplitude $0 \leq \frac{\mathcal{A}}{2b} \ll 1$. The absolute minima of the effective potential correspond to the possible stable final chemical states. From the sequence of curves in Fig. 2, corresponding to $\frac{\mathcal{A}}{2b} = 0.0, 0.05, 0.1, 0.2$ and 0.3 , we see that increasing the noise amplitude tends to racemize the system. The homochiral states $|\eta| = 1$ exist only in the absence of noise (bottom curve). For low levels of noise, the system has stable chiral states corresponding to $|\eta| < 1$. For noise above a critical value, the only stable final state is the racemic solution $\eta = 0$ (top curve). Applying a linear stability analysis to Eq.(5) we calculate the critical noise level \mathcal{A}_c above which the *racemic*

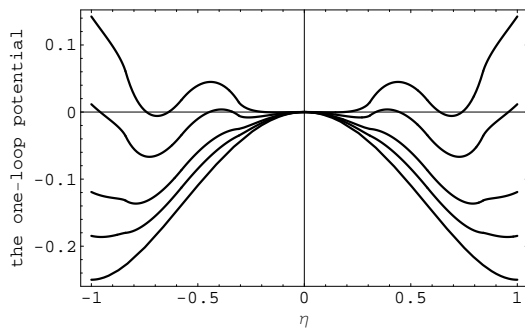


FIG. 2: The one-loop effective potential $V_{\mathcal{A}}/b$ for the Frank model. The final enantiomeric excess η , corresponds to the absolute minima of the potential, and decreases in absolute value below unity as the noise strength increases. The curves from bottom to top correspond to $\mathcal{A}/2b = 0.0, 0.05, 0.1, 0.2$ and 0.3 .

state is the globally stable solution: $\frac{\mathcal{A}_c}{2b} = \frac{1}{3} \cong 0.33$, which is borne out by inspection of the curves in Fig. 2. New relative maxima begin to form and persist for $\mathcal{A}/2b \gtrsim \mathcal{A}_c/2b$ thus leading to a pair of metastable chiral states (Fig. 2). Numerical simulations, in two and three dimensions [18], indicate however that the *ee* goes to zero continuously as the noise increases from zero and becomes strong, so these extra maxima are most likely artifacts of the lowest order calculation. Using the nominal values $k_3 \approx 10^2 \text{ Ms}^{-1}$, $k_{-2} \approx 10^{-5} \text{ Ms}^{-1}$ and $\chi^* = 1 \text{ M}$, then $2b = 100 \text{ s}^{-1}$, and external noises with $\mathcal{A} \lesssim 33 \text{ s}^{-1}$ would be perturbatively valid.

Chiral bias. External magnetic, electric, gravitational fields, and vortex motion, as well as polarized radiation, can induce mirror symmetry breaking [24]. Chiral bias can be studied via the potential by assigning chiral specific reaction rates to the monomer production and autocatalysis steps thus replacing k_i by $k_i^L = k_i(1 + \frac{1}{2}\epsilon)$ and $k_i^D = k_i(1 - \frac{1}{2}\epsilon)$ for $i = \pm 1, \pm 2$ where $k_i = (k_i^L + k_i^D)/2$ [18, 25]. For example, $\epsilon = \frac{\Delta E}{kT} \approx 10^{-17}$ for parity violation in the electroweak interactions at room temperature, where ΔE is the energy difference between the two enantiomers [25]. In the presence of chiral bias, the tree-level potential is given by (for $r = 0$) $\frac{V(\eta)}{b} = \frac{\eta^4}{4} - \frac{\eta^2}{2} - \epsilon'[\eta - \frac{\eta^3}{3}] + v_0$, where $\epsilon' = \epsilon \frac{(k_2 A - \frac{1}{2} k_{-2} \chi^*)}{(k_3 - k_{-2}) \chi^*}$. This is plotted in Fig. 3 for $1 > \epsilon' \geq 0$: Due to the tilt, there are no longer racemic solutions for any bias $\epsilon > 0$, only chiral states are possible, and only one of these two chiral states will be an absolute minimum; see also Fig. 1b of Gleiser and Walker [18]. When we include noise, the one-loop biased effective potential is obtained by subtracting $\epsilon'(\eta - \eta^3/3)$ from the right hand side of Eq.(12), and is valid up to terms of order $O(\epsilon' \mathcal{A})$ and $O(\mathcal{A}^2)$. At this lowest order, the effect of the bias is to tilt the noise corrected potential in the same sense as shown in Fig. 3, so that the sequence of noise induced minima located at $0 < \eta \leq 1$ in Fig. 2 now become the *absolute* minima. Due to this tilting the origin of the potential is no

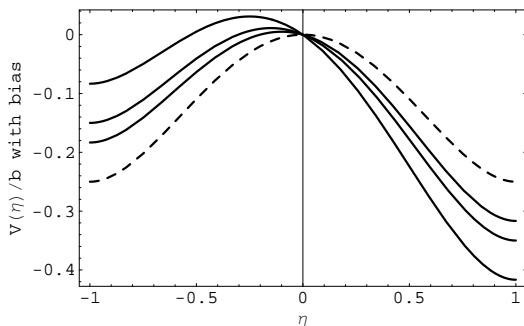


FIG. 3: Tree potential subject to small chiral bias. Dashed curve corresponds to zero bias. For $\epsilon' > 0$, the point $\eta = 1$ is the absolute minimum of the potential. For the sequence of solid curves below dashed curve, from top to bottom, $\epsilon' = 0.1, 0.2$ and 0.5 .

longer locally flat ($V'_A(0) \neq 0$) for any value of the noise. The noise has a racemizing effect upon the biased system such that above a critical noise level, the effective potential possesses a global minimum corresponding to a weakly chiral state. Thus for example, we calculate that for $\epsilon' = 0.001, 0.01$ and 0.1 then $\frac{A_c}{2b} = 0.311, 0.318$ and 0.388 , and the corresponding enantiomeric excesses are $\eta \approx 0.10, 0.15$ and 0.20 , respectively. For increasing chiral bias, ever stronger noise levels are “tolerated” before homochirality $|\eta| = 1$ is erased. A detailed account of noise and chiral bias on mirror symmetry breaking will

be provided elsewhere.

In this Letter we applied the stochastic field theory formalism of [21] to study the emergence of chirality in a key model of SMSB in chemistry in which environmental effects are modeled by external noise. We focused on the Frank model due to the central role it plays in theoretical approaches to mirror symmetry breaking [9, 11, 13, 14, 15, 16, 17, 18, 20, 22, 24, 25]. By strictly analytic means we verified that weak noise racemizes the system, erasing homochirality. This is a perturbatively valid key result, confirming the previous numerical results obtained by Gleiser and coworkers [18]. We also studied the competition between chiral bias and external noise and verified that stronger noise levels are required to racemize the system in the presence of bias. We assumed well-mixed conditions (zero dimensional systems), but the analytic method [21] enjoys the flexibility to include diffusion in d -dimensions and spatially dependent noise terms. A preliminary study of the $d = 2$ potential indicates that the results presented here carry over when spatial dependence is included. The important role that fluctuation phenomena, noise and chiral bias play in the origin of homochirality can therefore be analyzed in an elegant and systematic way.

We thank Josep M. Ribó and María-Paz Zorzano for useful discussions, and acknowledge the Grant AYA2006-15648-C02-02 from the Ministerio de Ciencia e Innovación (Spain).

-
- [1] P. Franck, W.A. Bonner and R.N. Zare, in *Chemistry for the 21st Century* eds. E. Keinan and I. Schechter (Wiley, Weinheim, 2000), p 175.
- [2] M. Avalos, R. Babiano, P. Cintas, J.L. Jimenez, J.C. Palacios and L.D. Barron, *Chem. Rev.* **98**, 2391 (1998).
- [3] J. Podlech, *Angew. Chem. Int. Edit.* **38**, 477 (1999); *Cell Mol Life Sci* **58**, 44 (2001).
- [4] I. Weissbuch, L. Leiserowitz and M. Lahav, *Top. Current Chem* **259**, 123 (2005).
- [5] W.A. Bonner, *Orig. Life Evol. Biosph.* **29**, 615 (1999).
- [6] A. Guijarro and M. Yus, *The Origin of Chirality in the Molecules of Life* (RSC Publishing, Cambridge, 2009).
- [7] S. Fox, *J. Chem. Educ.* **34**, 472 (1957).
- [8] J.L. Bada and S.L. Miller, *Biosystems* **20**, 21 (1987).
- [9] V.A. Avetisov, V.I. Goldanskii and V.V. Kuzmin, *Dokl. Akad. Nauk USSR* **282**, 115 (1985); V.I. Goldanskii, V.A. Avetisov and V.V. Kuzmin, *FEBS Lett.* **207**, 181 (1986); V. Avetisov and V. Goldanskii, *Proc. Natl. Acad. Sci. USA* **93**, 11435 (1996).
- [10] L.E. Orgel, *Nature* **358**, 203 (1992).
- [11] F.C. Frank, *Biochem. Biosphys. Acta* **11**, 459 (1953).
- [12] I. Gutman, D. Todorović and M. Vučković, *Chem. Phys. Lett.* **216** (1993) 447.
- [13] D.G. Blackmond, *Proc. Natl. Acad. Sci. USA* **101**, 5732 (2004).
- [14] P.G.H. Sandars, *Orig. Life Evol. Biosph.* **33**, 575 (2003).
- [15] A. Brandenburg and T. Multamäki, *Int. Jour. Astrobiol.* **3**, 209 (2004).
- [16] J.A. Wattis and P.V. Coveney, *Orig. Life Evol. Biosph.* **35**, 243 (2005).
- [17] Y. Saito and Hyuga, *J Phys Soc Jpn* **74**, 1629 (2005).
- [18] M. Gleiser and J. Thorarinson, *Orig. Life Evol. Biosph.* **36**, 501 (2006); M. Gleiser, *ibid* **37**, 235 (2007); M. Gleiser and S.I. Walker, *ibid* **38**, 293 (2008); M. Gleiser, J. Thorarinson and S.I. Walker, *ibid* **38**, 499 (2008).
- [19] W.H. Mills, *Chem. Ind. (London)* **10**, 750 (1932); K. Mislow, *Collect. Czech. Chem. Commun.* **68**, 849 (2003).
- [20] D. Hochberg and M.-P. Zorzano, *Chem. Phys. Lett.* **431**, 185 (2006).
- [21] D. Hochberg, C. Molina-París, J. Pérez-Mercader and M. Visser, *Phys. Rev. E* **60**, 6343 (1999); *Jour. Stat. Phys.* **99**, 903 (2000); *Physica A* **280**, 437 (2000); *Phys. Lett. A* **278**, 177 (2001).
- [22] D. Hochberg and M.-P. Zorzano, *Phys. Rev. E* **76**, 021109 (2007).
- [23] The exact endpoints are $\pm((6 \pm \sqrt{21})/15)^{\frac{1}{2}}$.
- [24] M. Avalos, R. Babiano, P. Cintas, J.L. Jimenez and J.C. Palacios, *Tetrahedron: Asymmetry* **11**, 2845 (2000).
- [25] D.K. Kondepudi and G.W. Nelson, *Physica A* **125**, 465 (1984).